International Journal of Future Generation Communication and Networking
Vol. 13, No. 4, (2020), pp. 4084–4094

RR-IQA Evaluation In View Of Image Denoising Using Subband Adaptive Filters

V. Balaji[1*], Ch.Anuradha[2], Dr. Patnala S.R. Chandra Murty[1]

[1] Department of Computer Science & Engineering, College of Engineering & Technology, Acharya Nagarjuna University, Guntur, Andhra Pradesh, India
[2] Department of Computer Science & Engineering, V. R. Siddhartha Engineering College, Vijayawada, Andhra Pradesh, India

([*]Corresponding Author Email: v.balaji.anu@gmail.com)

Abstract

Few of the images have deficient disparity along with significant kinds of artifacts. The elimination of artifact in images influenced by Gaussian white noise is a vital difficulty in diverse image processing and computer vision problems. Reduced-reference image quality assessment (RR-IQA) metrics are of high concern because in the most present and emerging practical real-world applications, the reference signals are not available. In this paper, we propose a new RR-IQA frame work constructed on adaptive subband decomposition-image denoising, in which the filter weights/coefficients are improved properly to a basic LMS strategy. By using perfect reconstruction property of filter bank (FB) decompositions we can design Subband adaptive filter (SAF). SAF modifies itself to the changing information conditions, denoising is additional efficacious compared to fixed filter banks. In this simulation the standard the multiply distorted image database (MDID-2013), images were employed to test the implementation of diverse SAF algorithms for image denoising to assess IQA metrics. The efficiency and execution of the methods of denoising are differentiated based upon the list of implement measures of image quality. Simulation outcomes states that the suggested mechanism outperforms the existing denoising procedures

Keywords: RR-IQA, LMS, SAF, FB, IQA, MDID

Introduction

Ongoing years have seen a gigantic development in procurement, transmission, and capacity of advanced media information. Subsequently, there has been an expanding interest for exact and productive picture and video quality appraisal measurements so as to monitor, keep up and store visual media data. Human visual framework is a definitive viewer of the visual media information. A commonplace visual media is dependent upon at least one handling stages, for example, securing/rendering, transmission, compression, among different procedures. Every one of these stages may change data and influence the nature of the visual information. It is important to keep up an acceptable nature of experience for viewers of visual data [1].

The most precise approach to pass judgment on the nature of pictures and recordings is to lead subjective analyses. Be that as it may, given the colossal measure of visual information, such analyses are very tedious. Thusly, programmed target picture/video quality assessment measurements that can imitate subjective assessment of visual information are of extraordinary intrigue. These computational models consider changes in visual information data just if these progressions cause irritation for viewers. The non-noticeable data changes in visual information are overlooked by these measurements [2].

Objective-IQA methods can be grouped into full-reference (FR), reduced-reference (RR) [3], and blind-reference (NR) [4] depending on their approach to the reference image with immaculate quality. Figure.1 provides an illustration of this categorization. Both reference image and possibly distorted image are accessible for a FR-IQA metric. RRIQA replicas have full access to the distorted image and carry out assessments with respect to some definite statistical attributes of the reference picture. To achieve quality evaluation of a possibly distorted image, RR-IQA models have no ingress to the reference image [3].

ISSN: 2233-7857 IJFGCN

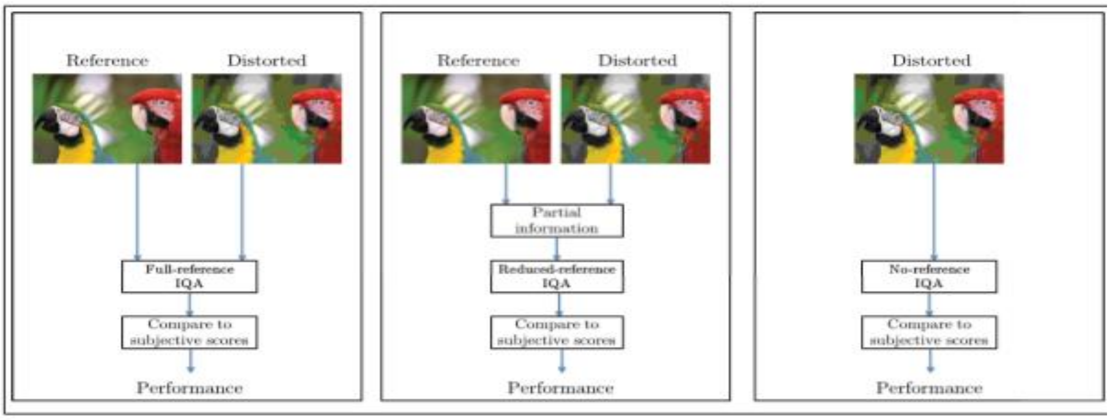

Figure.1 Category of IQA methods

The objective IQA is a multidisciplinary field with a broad scope of investigation directions at the convergence of signal and image processing, computer vision, visual psychophysics, neural physiology, information theory, ML&AI, design of image acquisition, communication, and show frameworks. IQA methods can be operated in parallel with an image processing system to yield feedback for the system or can be directly embedded into the system. Performance of a recognition system for an application can be considerably strained by image artifacts/distortions. Objective IQA can help to predict performance expectation of a recognition system or can give information to preprocess the input image first and run the recognition system on the processed image [2].

Generally images pickup artifact/noise in course of image acquisition and transmission procedure [5]. In image acquisition using a camera, the quantity of artifact/noise is acutate due to the extremity levels and sensor temperature. The interference in the transmission channel also persuades the artifact/noise in an image during transmission. This kind of noise is added substance in nature and is known as AWGN. The artifact in image poses problems for visual quality and automated analysis operations. In the process of the artifact are eliminated from the image while holding of important features. The important features like edges, textures etc are also disturbed during the image denoising. This alters the perceptible quality of the image. The attribute of the edges has the great important for the perceptible network. So the edge preserving during the image denoising is the essential preprocessing of the image processing.

The image denoising or adaptive noise cancellation (ANC) scheme, illustrated in Figure.2, ANC is a powerful technique for recovering a signal altered by additive noise and it is a principle key section of the signal processing. Figure.2 shows the essential problem and therefore the adaptive noise cancelling solution. The first input ***d(l)*** to the canceller is composite of a clean original signal ***s(l)*** from the signal source that's corrupted by the presence of a artifact $\boldsymbol{n_0(l)}$ which uncorrelated with the signal i.e. $\boldsymbol{s(n) + n_0(l)}$. The referenced input endures a noise $\boldsymbol{n_1(l)}$ uncorrelated with the signal but correlated with the noise $\boldsymbol{n_0(l)}$ This noise estimate is subtracted from the corrupted signal to supply an estimate of the signal is that the ANC system output ***y(l)***[5].

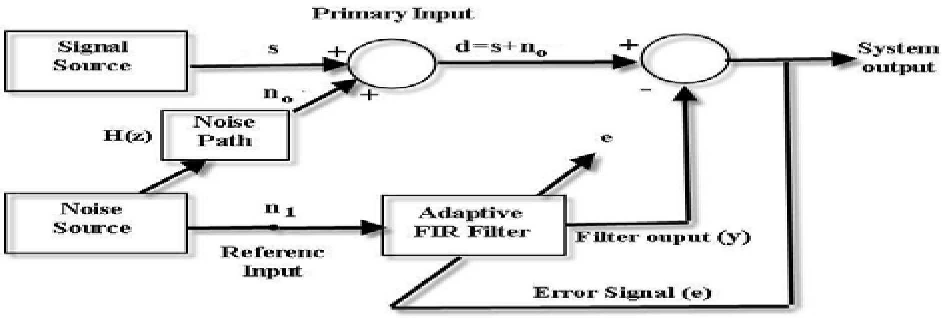

Figure.2 ANC block diagram

The AWGN and image edges are always presented by high frequencies. In this research work, a new RR-IQA procedure based on adaptive subband decomposition-image denoising is demonstrated. The few denoising techniques, fixed wavelet transform (FWT) is utilized to operate the whole image.

ISSN: 2233-7857 IJFGCN

The prime scheme of this research work is to use filter banks alternative of FWT to operate the distorted image.

Quadrature mirror filter (QMF) bank means quadrature (4 filters) *i.e*, two filters in analysis section($H_0$and H_1) and two filters in synthesis section(F_0 and F_1). Prototyping of any one of the 4 filters and remaining 3 filters are mirror image of that filter. QMF bank has broadly employed for splitting a sign into two or more sub bands in frequency domain, so each sub band signal is operated in an independent approach and adequate compression is additionaly performed. This sub band signals are recombined in properly reconstructed to create the signal very nearer to the primary signal [6].

QMF banks can be developed either perfect reconstruction (PR) or near perfect reconstruction (NPR) property, filter bank (FB) section can be cascaded in tree structure to create multilevel or multichannel FB. There are two kinds of tree structure designs, namely, uniform filter banks (UFB) structures and non-uniform filter banks (NUFB) structures. In UFB at every level, the low pass(LPF) and high pass filters(HPF) are split into two sections, whereas, only low pass filter splits into two sections in NUFB [17].

The structural description of two channel FB is presented in Figure.3 the digitalsignal ***u(l)*** is divided into 02 subbands having identical range of frequency of LPF and HPF analysis filters $\boldsymbol{H_0(Z)}$ and $\boldsymbol{H_1}$**(Z)** particularly. To diminish the computational complexity sub band signals are decimated by a factor 02. The decimated signals are normally digitally coded and imparted. At the synthesis part, the two sub band signals are decoded and the interpolated by a factor of two and ultimately organized between low pass and high pass filters $\boldsymbol{F_0}$**(Z)** and $\boldsymbol{F_1}$**(Z)** particularly. The out puts of synthesis filters are merged to procure the reconstructed signal ***y(l)***=$\boldsymbol{\hat{u}(l)}$.

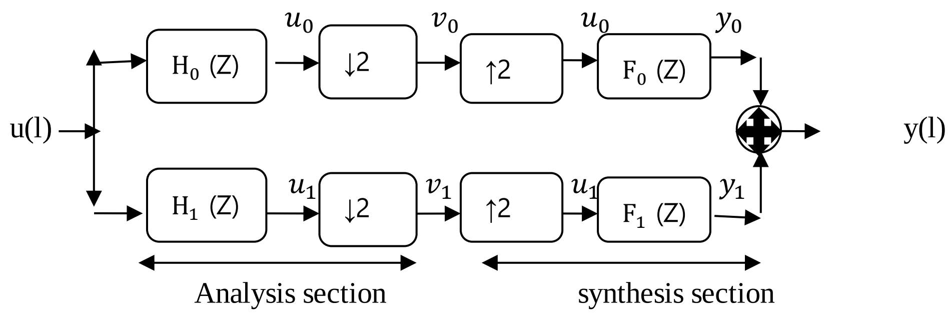

Figure.3 Two Channel- Filter Bank

The postulations of the adaptive FB (AFB) are organized in [6]. Elegant adaptive estimation hypothesis are integrated PR with FB i.e. PRFB in [6]. In [1] these structures are used for image coding during which the filters fits the non-stationary input states consistent with an adaptation scheme like the essential least mean square algorithm. Since AFB adapt to the alerting input conditions denoising is more advantageous differentiated to the systematic fixed FB. In our framework, the upper division/branch is that the low pass filtered and down sampled version of the first signal, and also the lower division/branch signal is primarily the adaptive estimation error. within the QMF the samples of the lower division/branch is adaptively estimated using the samples of the low pass filtered upper division/branch [6].

Materials and methods

Subband Adaptive Filter Banks

Subband adaptive filters (SAF) that are all the more computationally productive for applications that require a more drawn out channel length, and are progressively powerful if the input is exceptionally connected. This can be disservice of utilizing FIR systems for adaptive filtering because of the high computational burden and more slow convergence. An oversized portion of the suggested adaptive calculations for subband decomposition FB, give some thought to the difficulty of framework recognization and artifact/noise elimination [7]. The choice of SFB as per the knowledge signal is likewise examined by scholars [14]. The first objective of those research works is to find the most effective wavelet basis for decaying the entire information, and fixed filter banks picked by an

ISSN: 2233-7857 IJFGCN

optimality measure are utilized in the course of the entire term or degree of the signal though the filters vary because the idea of the input changes [8].

Our adaptation theme is totally different from the SAF structures that perform AF within the subbands. The adaption theme in our methodology neither tries to estimate AN unknown system nor uses a fixed FB throughout the whole period of the signal. Our theme inherently updates the FB and finds ideal filters for each signal sample whereas conserving the PR property, as long because the identical adaptation strategy is used throughout the analysis and synthesis. Therefore, no facet info must be transmitted for PR. this is often an enormous property of the FB in image denoising applications, as a results of adaptive filter coefficients are often hold on and reused throughout reconstruction [9].

The FB segments the signal into various subbands that possess coterminous bits of the waveband. In SAF the signaling is deteriorated into various parrallel channels. The SAFs are based upon multirate computerized FB, which include down sampling process and up sampling procedure areas. By dividing the fullband input and desired input signals into various subband signals, individual adaptive sub filters will be applied to their separate subband signals to boost system framework execution.

Proposed Frame Work

The AF can examine the signal at various frequencies with various resolutions. So SAF based denoising in pictures has been a well known research work in the previous few years. Data base images/ pictures regularly ruined by artifacts because of certain components, for example, machine specifications and environmental factors. The basic proposed frame work for RRIQA Evaluation based on image denoising and histogram is shown in Figure.4

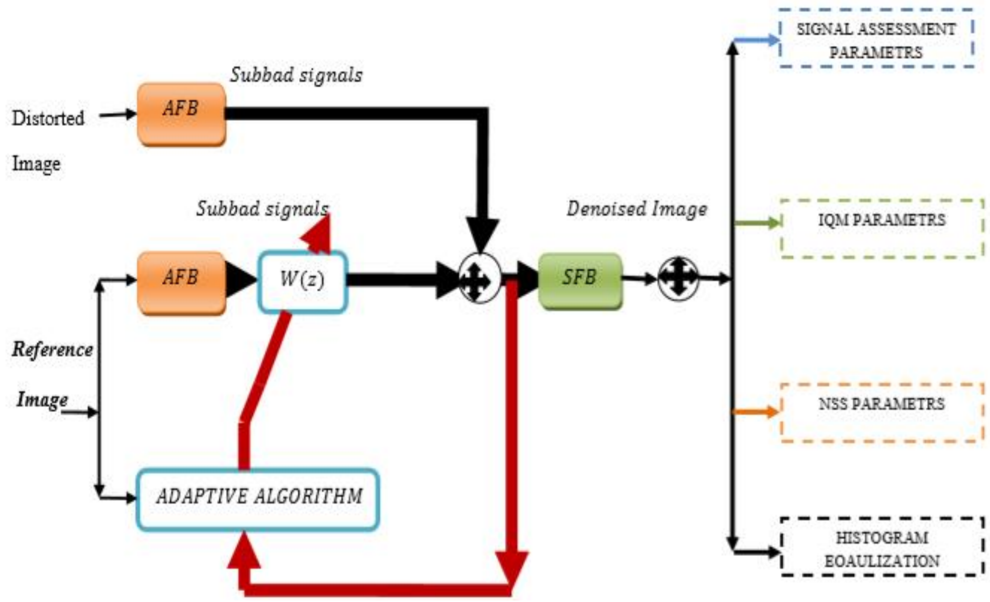

Figure.4: Proposed Frame work block diagram

The artifact elimination procedure, modeled as follows: Suppose ***s(l)*** be a original reference image and ***d(l)*** be artifact corrupted image with AWGN $n_0(l)$ used in equation 1;

$$d(l) = s(l) + n_0(l) \qquad (1)$$

The full band reference sign u(l) and first input desired response d(l) are decomposed into N spectral bands using analysis filters Hi(z), i = 0, 1,...,(N – 1). These subband signals are decimated to a lower rate using the identical factor N and are processed by individual adaptive sub filters Wi(z). Each sub filter has an independent adaptation loop with a locally computed error signal ei,D(k) for updating the faucet weights to reduce the corresponding subband error signal. The fullband error signal e(l) is finally obtained by interpolating and recombining all the subband error signals employing a synthesis filter bank. Notice that the variable l is that the time index for the fullband signals and k is that the time index for the decimated subband signals [9].

The decimation factors must fulfill the following condition [6] for basic design structure of ***N***-band UFB approach having decimation N_0, $N1$, $N2$---N_{N-1} for each band.

ISSN: 2233-7857 IJFGCN

$$\sum_{k=0}^{N-1} \frac{1}{N_k} = 1 \quad (2)$$

The PR condition for ***N***-band UFB is achieved by using following equation

$$\sum_{k=0}^{N-1} |H_k(z)|^2 = 1 \quad \text{for } 0 \le w \le \frac{\pi}{N} \quad (3)$$

Here $H_k(z)$ is transfer function of k^{th} filter in UFB.

To evaluate performance of SAF's various UFB structures such as 3 level decomposition *i.e* three band FB with decimation factors (3,3,3) (**TBFB**), 4 level decomposition *i.e* four band FB with decimation factors (4,4,4,4) (**FBFB**), and 5 level decomposition *i.e* five band FB with decimation factors (5,5,5,5,5) (**FVBFB**) using different adaptive algorithms are implemented [6]. The proposed frame work can be explained UFB structures with 3 level decomposition. *i.e* **TBFB** is shown in Figure.5

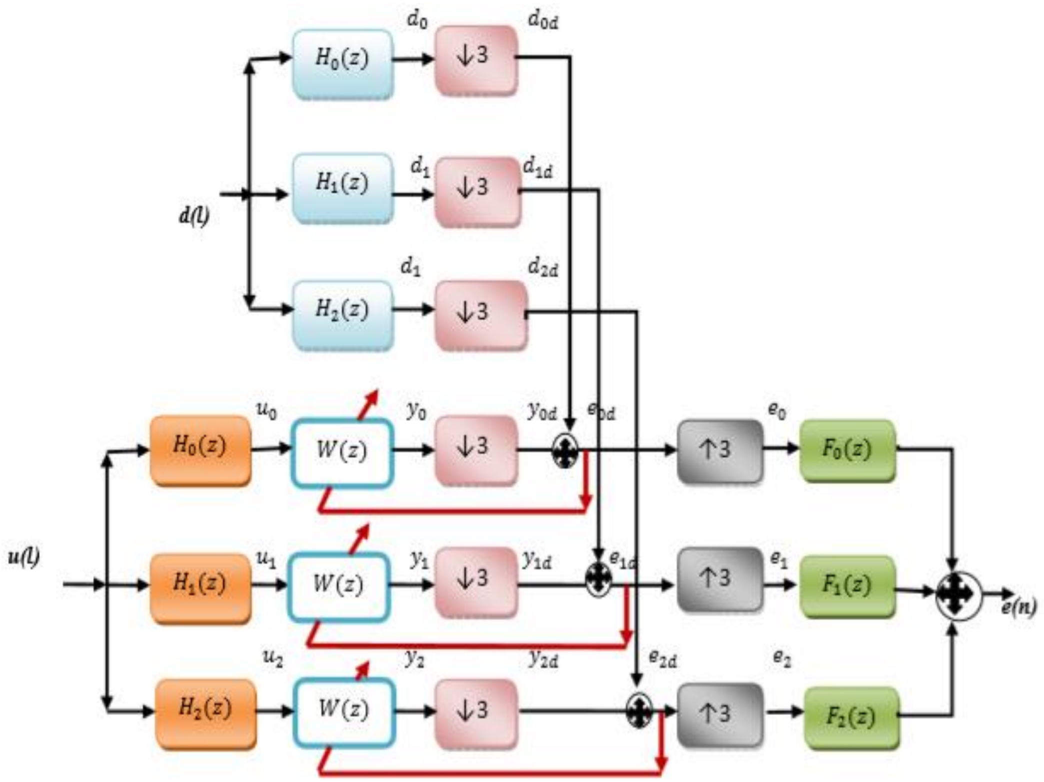

Figure.5: Proposed Uniform Filter Bank structured SAF

The PR condition for proposed UFB based **TBFB** can be achieved by using following equation

$$|H_0(z)|^2 + |H_1(z)|^2 + |H_2(z)|^2 = 1 \quad \text{for } 0 \le w \le \frac{\pi}{3} \quad (4)$$

Here *$H_0(z)$ and $H_1(z)$* analysis filters are LPF (low pass filters) in the first and second stages and $H_2(z)$ is HPF(high pass filter) last stages.

The traditional ANC shown in Figure.2 incorporates filter whose input parameters are ***d(l)*** and ***u(l)***. Here ***u(l)*** and ***w(l)*** are reference input signal array and adaptive filter coefficients respective given below

$$u(l) = [u(l), u(l-1), u(l-2), \ldots\ldots\ldots u(l-M+1)]^T \quad (5)$$

$$w(l) = [w_0(l), w_1(l), w_2(l), \ldots\ldots\ldots\ldots w_{M-1}(l)]^T \quad (6)$$

Figure.5 shows two identical structures for the chose input part of the subband adaptive framework as shown that the full band adaptive filter ***W(z)*** of length ***M*** [6]. The required computational steps in every iteration as takes after for ***N*** sub bands of SAF algorithms are shown in following equations. The time index of original sequence is noted as ***l*** and ***k*** represents decimated signal time index.

The proposed FB based SAF cost function (error signal) is defined as

ISSN: 2233-7857 IJFGCN

$$e_D(k) = d_D(k) - U^T(k)w(k) \qquad (7)$$

Here $d_D(k)$ is N X 1 decimated primary signal (desired response) array and $U(k)$ is reference input sub band signal matrix with size M X N defined as follows

$$U(k) = [u_0(k), u_1(k), u_2(k), \ldots\ldots\ldots u_{N-1}(k)] \qquad (8)$$

$$d_D(k) = [d_{0,D}(k), d_{1,D}(k), d_{2,D}(k), \ldots. d_{N-1,D}(k)]^T \qquad (9)$$

The maximum optimal solution for SAF shown in Figure.4 is obtained after a adequate number of iterations with updated tap weight vector $w(k+1)$ in all N sub band signals sets $\{U(k), d_D(k)\}$at each iteration $\boldsymbol{k}$ as follows:

Basic Least Mean Square Algorithm

$$w(k+1) = w(k) + \alpha * u_i(k) * e_{i,D}(k) \qquad (10)$$

Here α is convergence rate parameter. The α value should be selected in $0 < \alpha < \frac{2}{N*P_u}$, where P_u is calculated as $u^T(l)u(l)$ *i.e* average power and N is number of sub bands.

Results and discussion

The benchmark the multiply distorted image database (MDID-2013), images [10] were chosen to test the execution of 3 types of subband decomposition schemes for image denoising. The MDID2013 is comprises of 12 reference pictures and 324 multiply distorted images three types of distortions (Gaussian blur, JPEG compression, and white Gaussian noise) and 03 distortion levels/type. These MDID-2013 data base images have a resolution of up to 1280 × 720.

The presented frame work has been simulated by using Parks-McClellan optimal equiripple linear phase low pass FIR filter of order 63. A low amplitude AWGN with variance 0.001 is generated for proposed denoising scheme. The same number of samples of AWGN noise as original image is considered. The data base images used for simulation are shown in below Figure.6. The computer simulation outcomes are procured for all data base images but only first and second images are presented in the figures (Figure.7 and Figure.8) for convenience. The similar strategy can be executed on MDID data base different images with various FB structured SAF's.

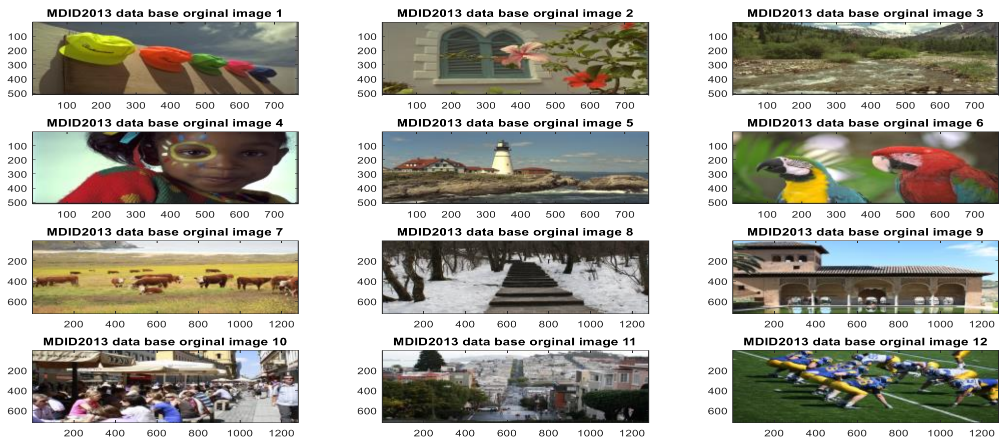

Figure.6 MDID-2013 database original reference images

Figure.7 Simulation results using four level decomposition filter bank (a) MDID data base original reference picture1 (b) Noise corrupted picture (c) Denoised picture using FBFB-SAF

ISSN: 2233-7857 IJFGCN

Figure.8 Simulation results using four level decomposition filter bank

(a) MDID data base original reference picture2 (b) Noise corrupted picture (c) Denoised picture

Signal-to-noise ratio (SNR) is also a quantity accustomed differentiate the extent of a primary information bearing signal to the quantity of artifact. The essential signal quality assessment metrics, signal-to-noise ratio before filtering (SNRBF) and SNR after filtering (SNRAF) for proposed frame work for image denoising are described within the subsequent equations [5].

$$SNRBF = 10\log_{10}\left(\frac{\sum_{n=0}^{N-1}[s(l)]^2}{\sum_{n=0}^{N-1}[d(l)-s(l)]^2}\right) \qquad (11)$$

$$SNRAF = 10\log_{10}\left(\frac{\sum_{n=0}^{N-1}[s(l)]^2}{\sum_{n=0}^{N-1}[e(l)-s(l)]^2}\right) \qquad (12)$$

Where ***s(l), d(l)*** and ***(el)*** are clean original reference, distorted and denoised images respectively.

To assess the performance of processed image, the Image Quality Measurement (IQM) plays a significant contribution. Quality of a image is defined as an attribute of an image that quantifies the processed image degradation by contrasting with perfect image. The list of IQM's used for proposed frame work are taken from [11] to evaluate the IQA performance comparison are listed in below Table.1

Table.1: Image Quality Assessment parameters for the proposed model

PARAMETERS	FORMULA
Mean Square Error	$MSE = \frac{1}{mn}\sum_{i=1}^{m}\sum_{j=1}^{n}(A_{ij} - B_{ij})^2$
Peak Signal to Noise Ratio	$PSNR = 10\log(\frac{255^2}{MSE})$
Normalized Cross − Correlation	$NCC = \sum_{i=1}^{m}\sum_{j=1}^{n}\frac{A_{ij} * B_{ij}}{A_{ij}^2}$
Average Difference	$AD = \frac{1}{mn}\sum_{i=1}^{m}\sum_{j=1}^{n}[A(i,j) - B(i,j)]$
Structural Content	$SC = \frac{\sum_{i=1}^{m}\sum_{j=1}^{n}(A_{ij})^2}{\sum_{i=1}^{m}\sum_{j=1}^{n}(B_{ij})^2}$
Maximum Difference	$MD = Max(\lvert A_{ij} - B_{ij}\rvert)$
Normalized Absolute Error	$NAE = \frac{\sum_{i=1}^{m}\sum_{j=1}^{n}(\lvert A_{ij} - B_{ij}\rvert)}{\sum_{i=1}^{m}\sum_{j=1}^{n}A_{ij}}$

Where $\boldsymbol{A}_{ij}$ is reference image pixel value with a size (***mxn***)

$\boldsymbol{B}_{ij}$ is processed image pixel value with a size (***mxn***)

Table.2 Signal quality comparison of the proposed technique

TY FB	**TBFB-SAF**				**FBTB-SAF**			**FVBFB-SAF**		
DB	**SNR BF**	**SNR AF**	**PSNR**	**MS E**	**SNR AF**	**PSN R**	**MSE**	**SNR AF**	**PSN R**	**MS E**
Im1	5.79	12.7 7	77.33	0.00	12.78	77.64	0.00	12.67	76.96	0.00
Im2	6.23	13.2 0	74.89	0.00	13.21	76.48	0.00	13.11	74.79	0.00

ISSN: 2233-7857 IJFGCN

Im3	6.46	13.44	69.14	0.01	13.45	69.41	0.01	13.35	69.11	0.01
Im4	7.82	14.79	76.04	0.00	14.80	76.91	0.00	14.69	75.93	0.00
Im5	7.01	13.98	72.53	0.00	13.99	73.07	0.00	13.89	72.44	0.00
Im6	6.59	13.56	77.11	0.00	13.57	77.89	0.00	13.47	76.76	0.00
Im7	9.64	16.61	76.06	0.00	16.61	77.14	0.00	16.50	75.80	0.00
Im8	8.37	15.34	74.23	0.00	15.34	75.66	0.00	15.24	74.12	0.00
Im9	9.11	16.08	72.34	0.00	16.08	73.29	0.00	15.98	72.28	0.00
Im10	8.88	15.85	73.19	0.00	15.85	75.47	0.00	15.75	73.15	0.00
Im11	7.62	14.59	74.20	0.00	14.59	75.90	0.00	14.49	74.10	0.00
Im12	5.02	12.01	74.10	0.00	12.01	75.84	0.00	11.92	74.01	0.00

Table.2 compares the signal quality assessment parameters of proposed technique in terms of SNRBF, SNRAF, PSNR and MSE parameters. From the Table.2, it is clear that the PSNR values obtained by using FBFB-SAF which has maximum when compared with other proposed methods. It is also evident that the minimum MSE values are obtained by using FBFB-SAF.

Table.3 Image Quality Assessment parameter values for proposed design

TYFB	**TBFB-SAF**				**FBTB-SAF**				**FVBFB-SAF**				
DB	**NCC**	**SC**	**MD**	**NAE**	**NCC**	**SC**	**MD**	**NAE**	**NCC**	**AD**	**SC**	**MD**	**NAE**
Im1	0.99	1.01	0.45	0.05	0.99	1.01	0.41	0.04	0.98	0.01	1.04	0.46	0.05
Im2	0.99	1.02	0.53	0.06	0.99	1.02	0.50	0.05	0.97	0.01	1.05	0.51	0.07
Im3	0.96	1.05	0.79	0.14	0.96	1.05	0.73	0.13	0.95	0.01	1.07	0.70	0.14
Im4	0.99	1.01	0.75	0.05	0.99	1.01	0.74	0.05	0.98	0.01	1.04	0.75	0.05
Im5	0.98	1.02	0.62	0.08	0.98	1.03	0.61	0.07	0.97	0.01	1.05	0.60	0.08
Im6	0.99	1.01	0.45	0.04	0.99	1.01	0.46	0.04	0.98	0.01	1.04	0.49	0.05
Im7	0.99	1.01	0.39	0.04	0.99	1.01	0.39	0.04	0.98	0.01	1.04	0.37	0.05
Im8	0.99	1.02	0.47	0.07	0.99	1.02	0.45	0.06	0.97	0.01	1.04	0.50	0.07
Im9	0.98	1.02	0.64	0.07	0.99	1.02	0.65	0.06	0.97	0.01	1.05	0.67	0.07
Im10	0.99	1.02	0.55	0.06	0.99	1.02	0.51	0.05	0.97	0.01	1.04	0.54	0.07
Im11	0.99	1.02	0.67	0.07	0.99	1.02	0.52	0.06	0.97	0.01	1.05	0.53	0.07

ISSN: 2233-7857 IJFGCN

Im12	0.98	1.03	0.56	0.09	0.98	1.03	0.57	0.08	0.97	0.01	1.05	0.58	0.09

The performance are show in Table.3 of proposed techniques in terms of NCC, AD, SC, MD, and NAE parameters. From the Table.3 by using FBFB-SAF which has maximum NCC value and minimum MD and NAE values when compared with other proposed methods. It is also observed that the minimum AD and SC values are obtained by using TBFB-SAF.

The Pearson linear correlation coefficient (PLCC), Spearman rank-order correlation coefficient (SROCC) and root mean squared error (RMSE) are three generally used natural scene statistics (NSS) parameters which are employed to evaluate the competing IQA metrics [12]. The PLCC, SROCC and RMSE parameter values are obtained for proposed frame work are shown in Table.4

Table.4 The Natural Scene Statistics (NSS) parameters

TY FB	**TBFB-SAF**			**FBTB-SAF**			**FVBFB-SAF**		
DB	**PLCC**	**SROCC**	**RMSE**	**PLCC**	**SROCC**	**RMSE**	**PLCC**	**SROCC**	**RMSE**
Im1	0.97	0.97	0.03	0.97	0.97	0.03	0.96	0.96	0.04
Im2	0.97	0.90	0.05	0.97	0.90	0.04	0.96	0.88	0.05
Im3	0.86	0.88	0.09	0.86	0.88	0.09	0.85	0.87	0.09
Im4	0.99	0.96	0.04	0.99	0.96	0.04	0.98	0.95	0.04
Im5	0.90	0.90	0.06	0.90	0.91	0.06	0.89	0.90	0.06
Im6	0.97	0.95	0.04	0.97	0.95	0.03	0.96	0.94	0.04
Im7	0.97	0.94	0.04	0.97	0.95	0.04	0.97	0.94	0.04
Im8	0.97	0.97	0.05	0.97	0.97	0.04	0.96	0.96	0.05
Im9	0.94	0.96	0.06	0.94	0.97	0.06	0.93	0.96	0.06
Im10	0.98	0.98	0.06	0.97	0.99	0.04	0.96	0.98	0.06
Im11	0.98	0.98	0.05	0.98	0.98	0.04	0.96	0.97	0.05
Im12	0.92	0.84	0.05	0.92	0.85	0.04	0.92	0.82	0.05

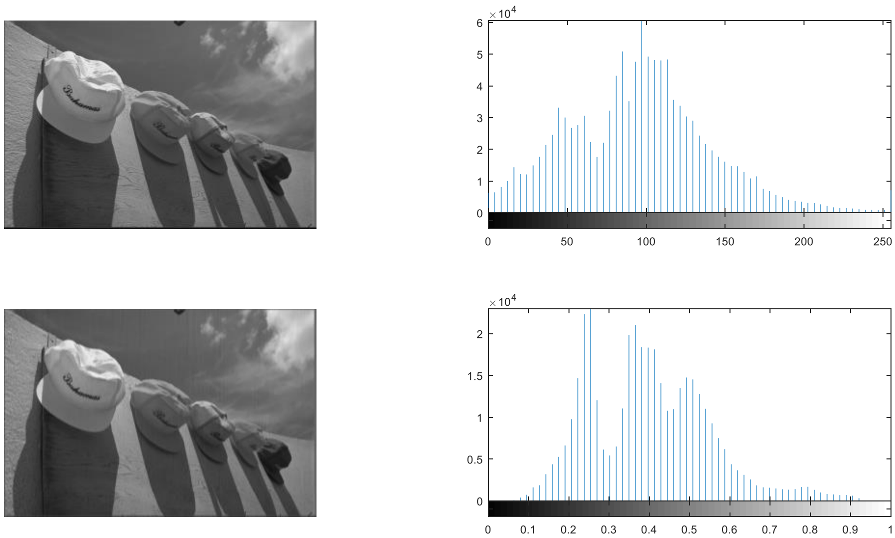

Figure.9 Histogram results using four level decomposition filter bank

(a) MDID data base original reference image 001(b) Reference image Histogram

(c) Denoised image using FBFB-SAF (d) Histogram of Denoised image

ISSN: 2233-7857 IJFGCN

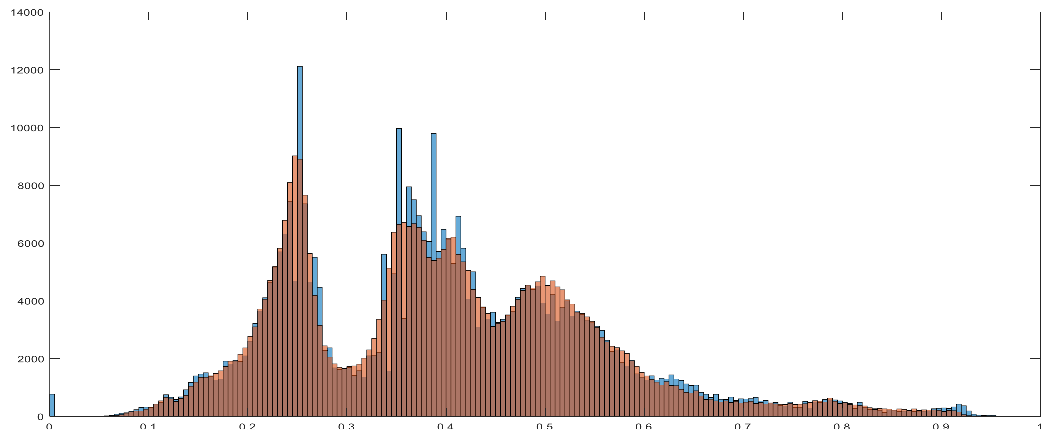

Figure.10 Histogram Equalization results using four level decomposition filter bank

Conclusions

We have introduced a hybrid frame work to estimate the reduced reference IQA using a subband adaptive filter bank decomposition approach. The fundamental contribution of this work is use of UFB with adaptive filtering strategy based on basic LMS algorithm for image denoising. The benchmark/standard MDID-2013 database was chosen to simulate the performance of the proposed design. Three level, four level and five level filter bank decompositions are considered to analyze performance comparisons of RR-IQA. The presented method input parameters are artifact/noise corrupted image (primary input) and AWGN noise (secondary input) for which processed/denoised image is obtained as output parameter. The performance evaluation of proposed frame work are compared on the basis of IQA parameters *i.e* MSE, PSNR, NCC, AD, SC, MD, NAE and NSS parameters such as PLCC,SROCC, RMSE. From the simulation results, demonstrates that the proposed four level FB decomposition structured SAF using LMS algorithm achieves good performance.

References

[1] Lee, Chulhee, et al. "Objective video quality assessment." *Optical engineering* 45.1 (2006): 017004.

[2] Li J, Li X, Yang B, Sun X. Segmentation-based image copy-move forgery detection scheme. IEEE transactions on information forensics and security. 2014 Dec 18;10(3):507-18.

[3] Ma, Jian, et al. "Reduced-reference stereoscopic image quality assessment using natural scene statistics and structural degradation." *IEEE Access* 6 (2017): 2768-2780.

[4] Wang, Shiqi, et al. "A patch-structure representation method for quality assessment of contrast changed images." *IEEE Signal Processing Letters* 22.12 (2015): 2387-2390.

[5] Bernard Widrow et al. "Adaptive noise cancelling: Principles and applications". In: Proceedings of the IEEE 63.12 (1975), pp. 1692–1716..

[6] Vaidyanathan, P. P. (2006). *Multirate systems and filter banks*. Pearson Education India.

[7] Bhandari, Ashish Kumar, et al. "Optimal sub-band adaptive thresholding based edge preserved satellite image denoising using adaptive differential evolution algorithm." *Neurocomputing* 174 (2016): 698-721.

[8] Kalavathy, S., and S. Suganthi. (2017) "Image Denoising Analysis Using Adaptive SubbandThresholding and Wavelet Packet." *Proceedings of the International Conference on Intelligent Computing Systems (ICICS 2017–Dec 15th-16th 2017) organized by Sona College of Technology, Salem, Tamilnadu, India*.

[9] Lee, K. A., Gan, W. S., & Kuo, S. M. (2009). *Subband adaptive filtering: theory and implementation*. John Wiley & Sons.

[10] Sun, W., Zhou, F., & Liao, Q. (2017). MDID: A multiply distorted image database for image quality assessment. *Pattern Recognition*, *61*, 153-168.

ISSN: 2233-7857 IJFGCN

[11] Memon, Farida, Mukhtiar Ali Unar, and SheerazMemon. "Image quality assessment for performance evaluation of focus measure operators." *arXiv preprint rXiv:1604.00546* (2016).
[12] Mittal, A., Moorthy, A.K. and Bovik, A.C., 2012. No-reference image quality assessment in the spatial domain. *IEEE Transactions on image processing*, *21*(12), pp.4695-4708.

ISSN: 2233-7857 IJFGCN